Recognition of Exogenous and Endogenous Nitroxyl in Living Cells via a Two-photon Fluorescent Probe

Haidong Li, Qichao Yao, Feng Xu, Ning Xu, Xuechao Ma, Jiangli Fan, Saran Long, Jianjun Du, Jingyun Wang, and Xiaojun Peng

Anal. Chem., **Just Accepted Manuscript** • DOI: 10.1021/acs.analchem.7b05172 • Publication Date (Web): 08 Mar 2018

Recognition of Exogenous and Endogenous Nitroxyl in Living Cells *via* a Two-photon Fluorescent Probe

Haidong Li,† Qichao Yao,† Feng Xu,† Ning Xu,† Xuechao Ma,† Jiangli Fan,† Saran Long,† Jianjun Du,† Jingyun Wang,‡ and Xiaojun Peng*†

†State Key Laboratory of Fine Chemicals, Dalian University of Technology, 2 Linggong Road, High-tech District, Dalian 116024, China. *Email: pengxj@dlut.edu.cn. Tel/Fax: +86 -411- 84986306.
‡Department School of Life Science and Biotechnology, Dalian University of Technology, 2 Linggong Road, High-tech District, Dalian 116024, China.

ABSTRACT: Nitroxyl (HNO), one electron reduced and protonated form of nitric oxide (NO), plays vital in various biological functions and pharmacological activities, such as mediating β-agonist dobutamine, inhibiting the activity of enzyme and treating cardiovascular diseases. However, the accurate mechanism of HNO in living cells is not thoroughly understood due to lacking of effective methods. In this work, a novel two-photon fluorescent probe **TP-HNO** was designed and synthesized based on 6-hydroxyl-quinonline-2-benzothiazole derivatives through introducing 2-(diphenylphosphino)benzoate as the ideal HNO recognition unit, which demonstrated the merits of outstanding selectivity, excellent sensitivity (DL 0.19 μM) and rapid response (20 min). In addition, owing to the high cell permeability and low biotoxicity of probe **TP-HNO**, it was successfully used for the qualitative and bioimaging of exogenous and endogenous nitroxyl concentration fluctuations in living cells via a two-photon laser confocal fluorescence microscopy, respectively, which is of importance for revealing the biological of HNO in the further.

INTRODUCTION

Nitroxyl (HNO), one electron reduced and protonated form of nitric oxide (NO), can be generated endogenously in living cells under the catalysis of nitric oxide synthase in appropriate conditions.[1, 2] It plays the unique roles in various biological functions and pharmacological activities,[2-4] which distinct from the birth of NO.[5-7] For instance, increasing numerous evidences have found that HNO is additive to the β-agonist dobutamine,[8] and could inhibit the activity of enzyme through reacting with thiols in aldehyde dehydrogenase,[9] and treat cardiovascular diseases by upregulating the calcitonin gene-related peptide (CGRP).[10,11] Besides, through activating voltage-dependent K^+ channel, HNO also could regulate the relaxation of resistant-like arteries in mammalian vascular systems.[12-14] In recent years, the investigation physiological function of HNO has gained more and more attention. However, the specific molecular mechanism of nitroxyl is not fully understood due to lacking of effective methods. Therefore, it is highly needed to develop the efficient method for monitoring HNO in biological system.

Owing to its high selectivity, excellent sensitivity, simple operation and well-defined spatiotemporal resolution, small-molecule fluorescent probes have been attracted tremendous attention.[15-23] Especially, compared with others analytical techniques such as colorimetric method,[24] mass spectrometry,[25] electron paramagnetic resonance,[26] high performance liquid chromatography[27] and electrochemical analysis,[28] it is more suitable for *in-suit* recognition of HNO in *vivo* without tedious sample pretreatments, time consuming and invasiveness characteristics.[29-38] Toward this end, some judiciously fluorescent probe have been designed to the detection of HNO in *vitro* or *vivo* depending on Cu(II)-based[39-42] or reaction-based method[43-51]. For examples, Lippard and cooperators fabricated some ingenious copper(II)-based probe **CuDHX1** to visualize HNO in mammalian cells for exploring the physiological processes.[52] Tan and Zhang's group reported probe **P-CM** for the quantitative detection of nitroxyl in bovine serum with satisfactory results.[53] Based on coumarin fluorophore, by introducing triphenylphosphonium salt as the mitochondria localization group, Kim and coworkers developed probe **Mito-1** for the sensing of HNO in mitochondria overcoming fluorescence interference form biothoils in cellular milieus.[44]

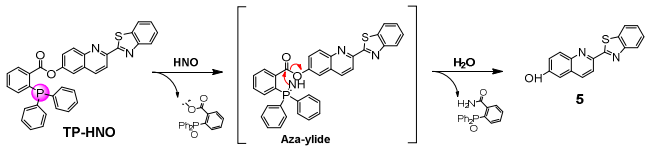

Scheme 1. Recognition mechanism of probe **TP-HNO** towards HNO

Chen and Yu *et al*. constructed a versatile fluorescence probe **Cyto-JN** based on azadipyrromethane fluorophore (Aza-BODIPY), which was applied for the detection and imaging intracellular HNO in living cells and mices.[54] Zhang *et al*. designed and synthesized a fluorescent chemodosimter **HNO-HBT** for the rapid detection of HNO in living cells.[48] Unfortunately, we found that most of reported fluorescent probes suffered from short excitation wavelength, interference from autofluorescence and photobleaching with one-photon irradiation. On the contrast, using near-infrared (NIR, 650-900 nm, coincident with the biological optical window) light as the excitation source, two-photon fluorescence probes having the prominent advantages, such as reducing photodamage, lowering self-absorption and increasing tissue penetration depth, had drawn more and more attentions in medical and biological research.[37,55-57] So far, there are few excellent performances two-photon fluorescent probe developed for the determination of HNO in *vivo*. Therefore, the aforementioned considerations inspire us to propose and synthesize a novel fluorescent probe for monitoring and bioimaging of HNO in complicated biological system under two-photon microscopy.

Hence, based on the excellent two-photon absorption cross section of 6-hydroxyl-quinonline-2-benzothiazole derivatives, [55, 58-60] we have developed a novel two-photon fluorescent probe **TP-HNO** through introducing 2-(diphenylphosphino)benzoate as an the ideal HNO recognition moiety. When the reagent (HNO donor) was added into PBS buffer solution, the fluorescence emission intensity of around 550 nm demonstrated an obvious enhancement within 20 min. Probe **TP-HNO** showed the exclusive selectivity of HNO overcoming interferences from biological reducants including glutathione. The sensing mechanism was verified by the High Resolving Mass Spectrum (HRMS). Furthermore, the detection limit of probe was calculated as low as 0.19 μM based on the principle of $3\sigma/k$, which showed that it was excellent sensitivity towards HNO in *vitro*. More importantly, owing to its high biocompatibility, low biotoxicity and good stability under physiological conditions, probe **TP-HNO** was successfully applied to recognize and image exogenous and endogenous nitroxyl in living cells through two-photon fluorescence microscopy.

EXPERIMENTAL SECTION

General information and materials

All reagents used were obtained from commercial suppliers and were used without further purification unless otherwise stated. Solvents used were purified *via* standard methods. Twice-distilled purified water used in all experiments was from Milli-Q systems. ^{1}H NMR and ^{13}C NMR spectra were recorded on a VARIAN INOVA-400 (or a Bruker Avance II 400 MHz or 500 MHz) spectrometer. Chemical shifts (δ) were reported as ppm (in $CDCl_3$ or DMSO-d_6, with TMS as the internal standard). Flash column chromatography was performed using silica gel (100-200 mesh) obtained from Qingdao Ocean Chemicals. Angeli's salt ($Na_2N_2O_3$, AS) was purchased from Cayman Chemical. Absorption spectra were recorded on a CARY 60 UV-Vis spectrophotometer in 10×10 mm quartz cell. Fluorescence spectra were performed on a VAEIAN CARY Eclipse fluorescence spectrophotometer (Serial No.MY15210003) in 10×10 mm quartz cell. Excitation and emission slit widths were modified to adjust the fluorescence intensity to a suitable range. Mass spectrometric data were achieved with HP1100LC/MSD MS and an LC/Q-TOF-MS instruments. All pH measurements were performed using a Model PHS-3C meter. The fluorescence quantum yields for compounds with Absolute PL Quantum Yield Spectrometer (HAMAMATSU C11347). Instruments used in cell imaging tests were carried out on Olympus FV1000-IX81 confocal microscopy (Olympus, Japan). Slight pH variations in the solutions were achieved by adding the minimum volumes of HCl or NaOH (1 M). The test system were performed in PBS buffer solution (0.01 M, pH 7.4 and 25 μM CTAB) in *vitro*. All the interferential reagents were prepared based on published literature.[23, 35, 37]

Determination of the detection limit

The detection limit (DL) was calculation based on the fluorescence titration of probe **TP-HNO** (10 μM) in the presence of AS reagent (0-20 μM). The fluorescence intensity of probe **TP-HNO** was measured and standard deviation of the blank measurement was achieved. The detection limit was calculated with the following equation:

$$\text{Detection limit} = 3\sigma/k$$

Where σ is the standard deviation of the blank measurement, k is the slope between the fluorescence intensity ($F_{545\ nm}$) versus various the different concentrations of AS reagent.

Determination of the quantum yield

The test method was operated according to the previous literature.[38]

Cell incubation

HeLa cells and RAW 264.7 cells were purchased from Institute of Basic Medical Sciences (IBMS) of the Chinese Academy of Medical Sciences. Cells were cultured in Dulbecco's modified Eagle's medium (DMEM, Invitrogen) supplemented with 10 % fetal bovine serum (Invitrogen). The cells were seeded in confocal culture dishes and then incubated for 24 h at 37 ºC under a humidified atmosphere

containing 5% CO_2.

Cytotoxicity assays

Measurement of cell viability was tested by reducing of MTT (3-(4, 5)-dimethylthiahiazo (-2-yl)-3, 5-diphenytetrazoliumromide) to formazan crystals using mitochondrial dehydrogenases. MCF-7 cells were seeded in 96-well microplates at a density of 1×10^5 cells/mL in 100 μL medium containing 10 % FBS buffer. After 24 h of cell attachment, the plates were then washed with 100 μL/well by PBS. The cells were then cultured in medium with 0, 1, 5, 10 and 20 μM of probe **TP-HNO** for 24 h, respectively. Cells in culture medium without probe **TP-HNO** were used as the control. Six replicate wells were used for each control and test concentration. 10 μL of MTT (5 mg/mL) prepared in PBS was added to each well and the plates were incubated at 37 ºC for another 4 h in a 5% CO_2 humidified incubator. The medium was then carefully removed, and the purple crystals were lysed in 200 μL DMSO. Optical density was determined on a microplate reader (Thermo Fisher Scientific) at 570 nm with subtraction of the absorbance of the cell-free blank volume at 630 nm. Cell viability was expressed as a percent of the control culture value, and it was calculated using the following equation:

Cells viability (%) = $(OD_{dye} - OD_{Kdye})/ (OD_{control} - OD_{Kcontrol}) \times 100$

Living cells imaging

HeLa cells and RAW264.7 cells were seeded in galass-bottom culture dishes at approximately concentration of 2×10^4 cells/mL and allowed to culture for 24 h at 37 ºC in a 5% CO_2 humidified incubator. Under the confocal fluorescence microscope (Olympus FV1000-IX81) with a 60 × objective lens, probe **TP-HNO** was excited at 405 nm (one-photon) and 730 nm (two-photon), whereafter, fluorescence emission from green channel (OP model: 500-580 nm; TP model: 520-560 nm) was gathered. Quantitative image analysis of the average fluorescence intensity of cells, determined from analysis of 9 regions of interest (ROIs) across cells.

The synthesis of probe **TP-HNO**

The synthesis of **1**. Aminophenol (2.18 g, 20 mM) was dissolved in 15 mL hydrochloric acid solution (6 M). The mixture was stirred at 100 °C for refluxing under N_2 protection. Afterwards, the crotonaldehyde (2.24 g, 32 mM, 2.64 mL) was gradually added through needle tube within 45 min. Then, the reaction system was continued to refluxing overnight. After cooling to room temperature and adjusting the pH to neutral, the mixture was extracted with ethyl acetate three times. The organic phase was dried with anhydrous Na_2SO_4 for overnight, and vacuum filter. Next, the crude product was purified through silica gel column chromatography to obtain 2.61 g product **1** (Yield 82%). ^{1}H NMR (400 MHz, DMSO-d_6) δ 9.86 (s, 1H), 8.02 (d, J = 8.4 Hz, 1H), 7.76 (d, J = 9.0 Hz, 1H), 7.26 (dd, J = 14.7, 5.4 Hz, 2H), 7.10 (s, 1H), 2.58 (s, 3H).

The synthesis of **2**. Compound **1** (318 mg, 2 mM) and K_2CO_3 (358.8 mg, 2.6 mM) were dissolved in 6 mL dry dimethyl formamide (DMF) solution. The reaction system was stirred at 80 °C for 30 min under N_2 protection, then, benzyl chloride (304 mg, 2.4 mM) was added via drop by drop strategy until the end. Afterwards, the mixture was continued to refluxing for 24 h. After cooling to room temperature, the mixture was extracted with ethyl acetate three times. The organic phase was dried with anhydrous Na_2SO_4 for overnight and vacuum filter. Next, the crude product was purified through silica gel column chromatography to obtain 2.61 g white product **2** (Yield 89%). ^{1}H NMR (400 MHz, DMSO-d_6) δ 8.13 (d, J = 8.4 Hz, 1H), 7.84 (d, J = 8.8 Hz, 1H), 7.52 (d, J = 7.4 Hz, 2H), 7.40 (dd, J = 22.0, 9.4 Hz, 6H), 5.22 (s, 2H), 2.61 (s, 3H).

The synthesis of **3**. Compound **2** (373.5 mg, 1.5 mM) was put into 30 mL 1, 4-dioxane in glass bottle. The mixture was stirred at 60 °C for 20 min. Afterwards, SeO_2 (233.1 mg, 2.1 mM) was added into reaction system by dropwise within 30 min. When aforementioned process was finished, the temperature was adjusted to 80 °C for stirring 4 h. After vacuum filter, the filtrate was obtained for needing further purification. The crude product was purified through silica gel column chromatography to obtain 250 mg yellow product **3** (Yield 63%). ^{1}H NMR (400 MHz, DMSO-d_6) δ 10.09 (s, 1H), 8.46 (d, J = 8.4 Hz, 1H), 8.16 (d, J = 9.0 Hz, 1H), 7.97 (d, J = 8.4 Hz, 1H), 7.76 -7.26 (m, 7H), 5.31 (s, 2H).

The synthesis of **4**. Compound **3** (263 mg, 1.0 mM) and 2-aminothiophenol (187.5 mg, 1.5 mM, 0.16 mL) were dissolved 4 mL dry dimethyl sulfoxide (DMSO). The reaction system was stirred at 130 °C for 6 h with N_2 protection. After cooling to room temperature, 10 mL water was added into glass bottle. Then, the mixture was extracted with ethyl acetate three times. The organic phase was dried with anhydrous Na_2SO_4 for overnight and vacuum filter. Next, the crude product was purified through silica gel column chromatography to obtain 239.2 mg greyish white product **4** (Yield 65%). ^{1}H NMR (400 MHz, DMSO-d_6) δ 8.48 (d, J = 8.6 Hz, 1H), 8.42 (d, J = 8.6 Hz, 1H), 8.20 (d, J = 7.8 Hz, 1H), 8.15 (d, J = 8.0 Hz, 1H), 8.07 (d, J = 9.2 Hz, 1H), 7.64 (d, J = 2.6 Hz, 1H), 7.58 (ddd, J = 18.2, 11.3, 6.0 Hz, 5H), 7.45 (t, J = 7.4 Hz, 2H), 7.39 (d, J = 7.2 Hz, 1H), 5.31 (s, 2H).

The synthesis of **5**. Compound **4** (280 mg, 0.76 mM) was fully dispersed in 7 mL dry dichloromethane (DCM) under ice bath condition. After stirring about 15 min, BBr_3-CH_2Cl_2 solution (1 M, 3.04 mL) was added via drop by drop until the end. Then, the mixture was stirred for 3 h at room temperature. Next, 10 mL water was added to quench reaction and pH value of solution was adjusted to 7 with $NaHCO_3$ solution. Then, the mixture was extracted with CH_2Cl_2 three times. The organic phase was dried with anhydrous Na_2SO_4 for overnight and vacuum filter. Next, the crude product was purified through silica gel column chromatography to obtain 90 mg pale yellow product **5** (Yield 43%). ^{1}H NMR (400 MHz, DMSO-d_6) δ 10.40 (s, 1H), 8.38 (d, J = 8.7 Hz, 1H), 8.34 (d, J = 8.6 Hz, 1H), 8.19 (d, J =

7.7 Hz, 1H), 8.13 (d, J = 8.0 Hz, 1H), 8.01 (d, J = 9.1 Hz, 1H), 7.65-7.55 (m, 1H), 7.52 (dd, J = 11.0, 4.1 Hz, 1H), 7.43 (dd, J = 9.1, 2.7 Hz, 1H), 7.27 (d, J = 2.6 Hz, 1H).

The synthesis of probe **TP-HNO**. Compound **5** (90 mg, 0.32 mM), 2-(diphenylphosphanyl) benzoic acid (153 mg, 0.5 mM), EDCI (95.9 mg, 0.5 mM) and DMAP (4 mg, 0.03 mM) were dissolved in 8 mL dry CH_2Cl_2 under N_2 protection. After stirring for overnight, 5 mL water was added into this reaction system. Then, the mixture was extracted with CH_2Cl_2 three times. The organic phase was dried with anhydrous Na_2SO_4 for overnight and vacuum filter. Next, the crude product was purified through silica gel column chromatography to obtain 40 mg white product **TP-HNO** (Yield 21%). ^{1}H NMR (400 MHz, DMSO-d_6) δ 8.57 (d, J = 8.6 Hz, 1H), 8.49 (d, J = 8.6 Hz, 1H), 8.33 (dd, J = 8.4, 4.0 Hz, 1H), 8.22 (d, J = 7.9 Hz, 1H), 8.17 (dd, J = 8.5, 3.4 Hz, 2H), 7.76 (d, J = 2.2 Hz, 1H), 7.69-7.50 (m, 5H), 7.42 (d, J = 3.5 Hz, 6H), 7.32-7.19 (m, 4H), 6.97 (dd, J = 8.4, 4.1 Hz, 1H). ^{13}C NMR (125 MHz, $CDCl_3$) δ 169.60 ,165.09, 154.29, 151.11, 149.18, 145.86, 141.63, 141.41, 137.49, 136.70, 136.45, 134.50, 134.17, 134.01, 133.14, 132.76, 131.44, 131.06, 129.22, 128.88, 128.64, 128.39, 126.30, 125.90, 125.38, 123.77, 122.02, 118.77, 118.53. ^{31}P NMR (162 MHz, $CDCl_3$) δ -3.81 (s, 1H). HRMS: m/z calcd for $C_{35}H_{23}N_2NaO_2PS^+$ $[M+Na]^+$: 589.1110, found: 589.1130.

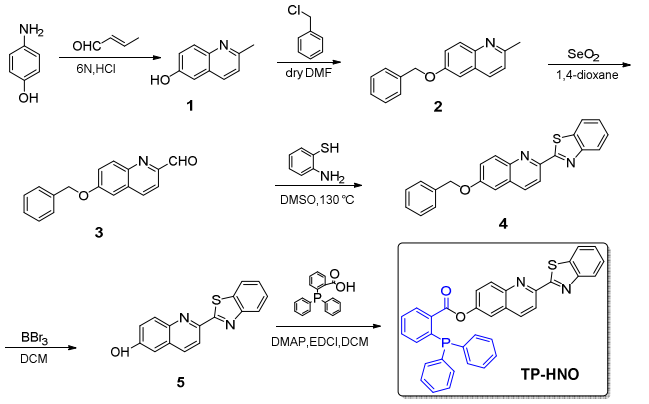

Scheme 2. Synthetic procedures of probe **TP-HNO**

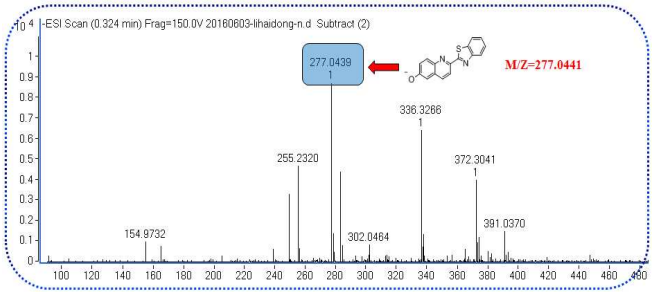

Figure 1. HRMS verification of probe **TP-HNO** for HNO

RESULTS AND DISCUSSION

Design probe TP-HNO and recognition mechanism. As shown in Scheme 2, the fluorescence probe **TP-HNO** was successfully synthesized through a multistep procedure. The intermediates of each step were characterized by nuclear magnetic resonance (^{1}H NMR, Figure S1-5). Besides, the target material **TP-HNO** was carefully confirmed by nuclear magnetic resonance (^{1}H, ^{13}C and ^{31}P NMR, Figure S6-8) and high resolution mass spectrum (HRMS, Figure S9) in the Supporting Information section. 6-hydroxyl-quinonline-2-benzothiazole (intermediate **5**) was a vital fluorophore, which had been proved to possess intrinsic two-photon absorption cross sections by Liu's group. [55, 58, 60] The maximum action two-photon absorption cross section ($\delta_{max}\Phi$) value of intermediate **5** was reported up to 50 GM (1 GM = 10^{-50} cm^4 s photon^{-1}) at 730 nm,[57] which demonstrated it was suitable for two-photon imaging in *vivo*. Moreover, 2-(diphenylphosphino)benzoate as the ideal HNO recognition moiety was chosen to install on intermediate **5** for constructing "potential" two-photon fluorescence probe **TP-HNO**. When HNO encountered probe **TP-HNO** in aqueous solution, it reacted with triphenylphosphine of probe to get the corresponding phosphine oxide and aza-ylide. Next, the aza-ylide went through a Staudinger ligation to obtain an amide derivate and intermediate **5** as the dual photon signal source. As the principle of probe **TP-HNO** sensing HNO was outlined in Scheme 1. In order to further verification the sensing mechanism of probe **TP-HNO** for HNO, the high resolving mass spectrum (HRMS) analysis was carried out. Obviously, one peak centered at m/z 277.0439 (calcd. 277.0441 for $C_{16}H_9N_2OS^-$) corresponding to deprotonation product [intermediate **5**]$^-$ was shown in Figure 1. Based on the above results, the sensing mechanism exactly was depicted in Scheme 1.

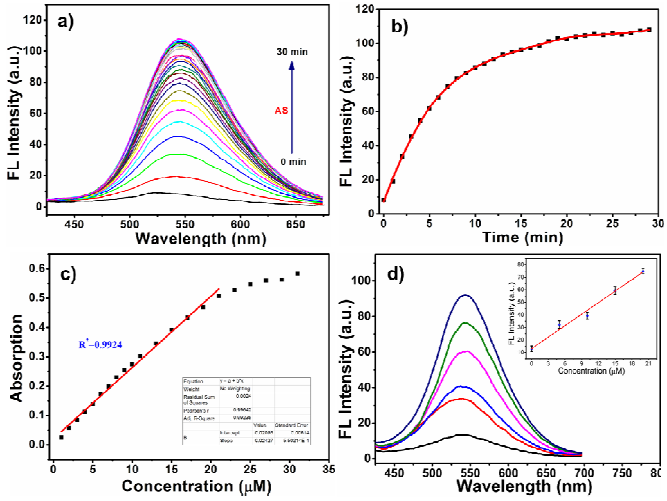

Figure 2. a) and b) Response time of probe **TP-HNO** towards HNO; c) the solubility of probe **TP-HNO**; d) fluorometric titration curve in PBS buffer solution (Insert: linearity of $F_{550\ nm}$ versus the different concentration of HNO). λex =363 nm, slit: 5/5 nm.

Response speed and spectroscopic characteristics. Initially, in order to evaluate the response speed of probe to HNO, the time-dependent (0-30 min) fluorescence responses of **TP-HNO** (5 μM) in the presence of 15 equiv

Angeli's salt ($Na_2N_2O_3$, AS), a precursor of HNO, were recorded every minute, as shown in Figure 2a. Upon addition of AS reagent in PBS buffer solution, the fluorescence emission center around 550 nm gradually enhanced with the excitation at 363 nm, signifying HNO triggered the cleavage of 2-(diphenylphosphino)benzoate from probe **TP-HNO** for releasing intermediate **5** signal part. From the Figure 2b, the fluorescence intensity of 550 nm wound not increase after 20 min, which indicated probe **TP-HNO** had the potential for real-time monitoring of HNO in biosystems. Next, we explored the fundamental photophysical properties of probe **TP-HNO**. The UV-Vis spectra and fluorescence spectra of **TP-HNO** in different solvents were demonstrated in Figure S10a and Figure S10b, respectively. In addition, the probe **TP-HNO** possessed a good solubility in testing system (Figure 2c and Figure S11). Fluorescent titration experiments were carried out to investigate the sensitivity of probe towards HNO. As shown in Figure 2d, the fluorescence emission intensity of 550 nm was plotted versus the concentration of AS reagent ranging from 0 to 20 μM, which exhibited an excellent linearity (R^2=0.9809). Thus, the detection limit was calculated as low as 0.19 μM based on the principle of $3\sigma/k$. Such low limit of detection demonstrated that probe **TP-HNO** was highly sensitive to HNO and could be acted as an effective tool for realizing the quantitative detection of HNO in *vitro*.

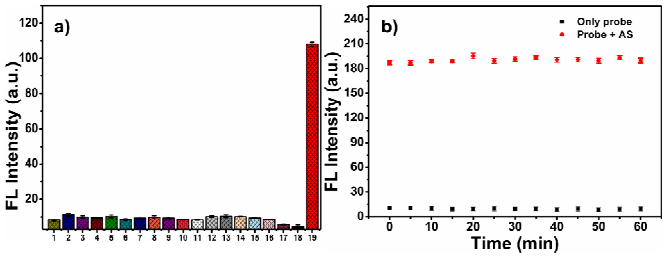

Figure 3. a) The selectivity of **TP-HNO** (5 μM) towards various analytes. Insert 1: blank; 100 equiv (2: K^+; 3: Na^+; 4: Ca^{2+}; 5: Mg^{2+}; 6: Zn^{2+}; 7: NO_3^-; 8: NO_2^-; 9: F^-; 10: HS^-;) 50 equiv (11: NaClO; 12: H_2O_2;) 100 equiv (13: Glutathione; 14: Cysteine;) 15: 250 equiv NO; 250 equiv (16: TBHP; 17: TBO•; 18: HO•;) 19: 15 equiv HNO and b) the stability of time dependence of **TP-HNO** (10 μM) with 15 equiv HNO (red line) or not (black line) in PBS buffer solution. λex=363 nm, slit: 5/5 nm.

Selectivity and stability of probe TP-HNO. The specificity selectivity of fluorescent probe determines its availability in actual sample. Therefore, we investigated the ability of probe **TP-HNO** to distinguish the HNO from various biological relevant species through fluorescence assay measurements in PBS buffer solution, such as ions (K^+; Na^+; Ca^{2+}; Mg^{2+}; Zn^{2+}; NO_3-; NO_2^-; F^-; and HS^-), nitric oxide (NO), oxidizing substance (NaClO, H_2O_2, TBHP, TBO•, HO•), and common amino acids (Cysteine and Glutathione). As depicted in Figure 3a, only adding AS reagent could induce a significant fluorescence enhancement at 550 nm, while others relative analytes exhibited no negligible the fluorescence changes of probe **TP-HNO**. Moreover, competitive experiments were also performed to estimate the availability of probe **TP-HNO** in complicated systems. No obvious interference was obtained towards aforementioned biological relevant species (Figure S12), indicating the potential applications of probe **TP-HNO** for detecting HNO in complex biological system. Whereafter, the stability of probe was also studied through fluorescence assay measurements in PBS buffer solution (Figure 3b) and in living HeLa cells (Figure S13), which indicated the possibility capability of this probe for long time imaging in physiological environment.

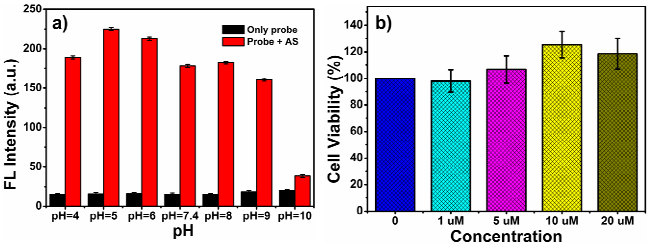

Figure 4. a) The pH effects of probe **TP-HNO** in PBS buffer solution and b) cytotoxicity assays of probe **TP-HNO** in living MCF-7 cells.

pH effects and cytotoxicity assays. Subsequently, the effects of pH on the recognition of probe **TP-HNO** (10 μM) for HNO (15 equiv) were carried out in PBS buffer solution. As shown in Figure 4a, probe **TP-HNO** demonstrated almost no changes in the fluorescence emission intensity of 550 nm in the range of pH 4.0-10.0, which indicated probe **TP-HNO** would not be depended on the acidity of the humoral environment. Upon addition 15 equiv HNO, the fluorescence emission intensity of 550 nm displayed distinct enhancement in PBS buffer solution of pH 4.0-9.0, clearly demonstrating the possibility capability of probe **TP-HNO** for imaging HNO in physiological pH microenvironment. Prior to cell tests, in order to study the biological cytotoxicity of probe **TP-HNO**, 3-(4, 5-dimethylthiazol-2-yl)-2, 5-diphenyltetrazolium bromide (MTT) assays in living human breast cancer cells (MCF-7 cells) with 0, 1, 5, 10 and 20 μM probe for 24 h were performed, respectively. The results showed almost nontoxicity of probe **TP-HNO** to cells at the concentration of 5 μM for 24 h under the experimental conditions (Figure 4b).

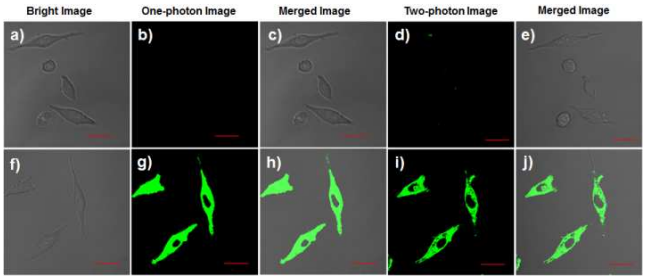

Figure 5. Exogenous nitroxyl imaging in RAW 264.7 living cells. One photon model: a) and f) bright channel; b) and g) green channel; c) and h) merged channel, λex=405 nm. Two

photon model: d) and i) green channel; e) and j) merged channel, λex= 730 nm, scale bar= 20 μm.

Exogenous nitroxyl imaging in living cells. Given the advantages of fluorescence probe **TP-HNO**, such as high selectivity, excellent sensitivity, low cytotoxicity, rapid response and working appropriately at the physiological pH, which made it have the possibility of imaging at the cellular level. So, cell imaging experiments were carried out upon one-photon and two-photon excitation model. As shown in Figure 5, RAW 264.7 cells were treated with 5 μM probe **TP-HNO** for 30 min at 37 °C in incubator, and no fluorescence signals in green channel (Figure 5b and 5d) were collected through one-photon (excitation with 405 nm) and two-photon (excitation with 730 nm) fluorescent microscopy, respectively. On the contrast, upon addition 30 μM AS reagent for cultivating another 30 minutes, obvious fluorescence signals in green channel (Figure 5g and 5i) were gathered, clearly indicating that probe **TP-HNO** could be used to monitoring exogenous nitroxyl imaging in living cells with excitation 405 nm (OP) and 730 nm (TP) via laser confocal fluorescence microscopy.

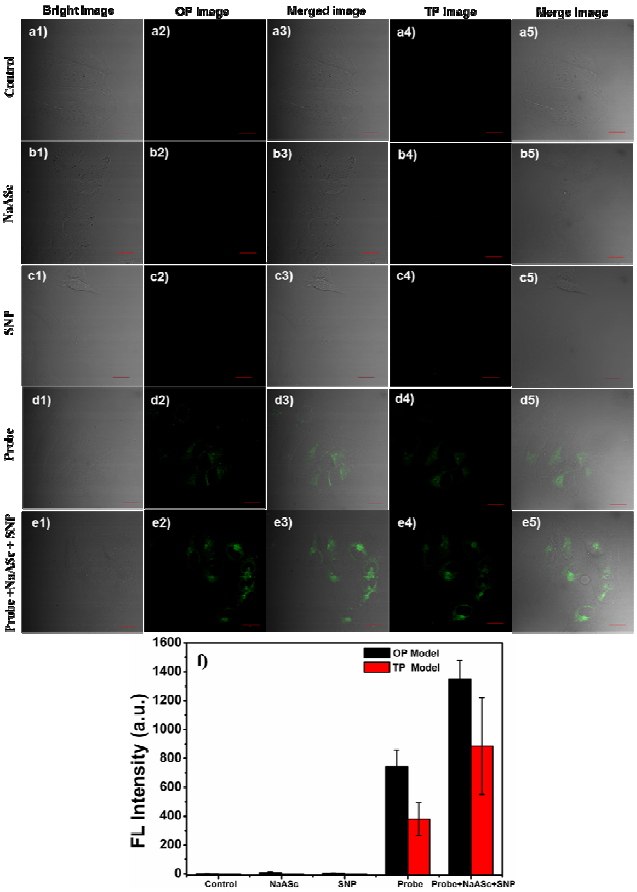

Figure 6. Endogenous nitroxyl two-photon imaging in living HeLa cells. a1-5) control group; b1-5) cells treated with 2 mM NaASc; c1-5) cells treated with 2 mM SNP; d1-5) cells treated with probe **TP-HNO**; e1-5) cells pre-treated with probe **TP-HNO** and then incubated with 2 mM NaASc and 2 mM SNP; f) green channel intensities were measured as averages of 9 regions of interest (ROIs) from different treated living HeLa cells. λex-OP =405 nm, λex-TP=730 nm, scale bar = 20 μm.

Endogenous nitroxyl imaging in living cells. Encouraged by the favorable property of probe **TP-HNO** for the exogenous nitroxyl imaging in living cells, we tried to study whether it possesses potential application for monitoring endogenous nitroxyl. Only adding 5 μM probe **TP-HNO** for 1 h in HeLa cells at 37 °C in incubator, there was weak fluorescent signal gathered from green channel with one-photon excitation at 405 nm (Figure 6d2) and two-photon excitation at 730 nm (Figure 6d4). Recently, Doctorovich and coworkers found that intracellular HNO could be formed through L-ascorbate reacting with NO in biological media.[61] Subsequently, the fluorescence intensity from green channel gradually brighten when HeLa cells were pretreated with 2.0 mM L-ascorbate (NaASc) and 2.0 mM sodium nitroprusside (SNP, NO donor) for another 2 h (Figure 6e2 and e4). And, with more stimulation cells through SNP, more intracellular HNO generated (Figure S14). By contrast, almost no fluorescent emission intensity of green channel were gathered (Figure 6a1-a5, 6b1-b5 and 6c1-5c5). Furthermore, the fluorescence intensities of each experimental group were extracted as averages of nine regions of interest (ROIs) (Figure 5f), which demonstrated probe **TP-HNO** could be competent for monitoring intracellular endogenous nitroxyl changes in living HeLa cells *via* with two-photon fluorescence microscope.

CONCLUSION

In conclusions, through rational design, we have proposed and synthesized a versatile two-photon fluorescent probe based on 6-hydroxyl-quinonline-2-benzothiazole derivatives. Probe **TP-HNO** demonstrated rapid response, high selectivity and excellent sensitivity for the recognition of HNO. The High Resolving Mass Spectrum (HRMS) analysis was carried out to verify the sensing mechanism of probe **TP-HNO** for HNO. In addition, probe TP-HNO also displayed high biocompatibility and it could be applied to bioimaging of exogenous and endogenous nitroxyl in living cells through two-photon laser confocal fluorescence microscopy. We anticipate that probe **TP-HNO** as a vital tool could be used to insight into the pathology and physiology biological effects of HNO in the further.

ASSOCIATED CONTENT

Supporting Information. ^{1}H-NMR, ^{13}C-NMR and ^{31}P-NMR spectra, HRMS spectra, absorbance and emission spectra and competitive experiments of probe **TP-HNO** are available in Supporting Information. This material is available free of charge on the ACS publications website.

AUTHOR INFORMATION

Corresponding Author

*Email: pengxj@dlut.edu.cn. Fax/Tel: +86 -411- 84986306.

Notes

The authors declare no competing financial interests.

ACKNOWLEDGEMENTS

This work was financially supported by National Natural Science Foundation of China (21376039, 21421005, 21422601 and 21576037), NSFC-Liaoning United Fund (U1608222) and National Basic Research Program of China (2013CB733702).

REFERENCES

(1) Miranda. K.M. *Coordin. Chem. Rev.* **2005**, 249, 433-455.
(2) Irvine,J.C.; Ritchie, R.H.; Favaloro, J.L.; Andrews, K.L.; Widdop, R.E.; Kemp-Harper, B.K. *Trends Pharmacol. Sci.* **2008**, 29, 601-608.
(3) Shafirovich, V.; Lymar. S.V. *P. Natl. Acad. Sci. USA* **2002**, 99, 7340-7345.
(4) Hamilton, K.; MacKenzie, A. *Vasc. Pharmacol*. **2015**, 71, 208-214.
(5) Hobbs, A.J.; Fukuto, J.M.; Ignarro, L.J. *P. Natl. Acad. Sci. USA* **1994**, 91, 10992-10996.
(6) Xu, W.; Liu, L.Z.; Loizidou, M.; Ahmed, M.; Charles, I.G.; *Cell Res.* **2002**, 12, 311-320.
(7) Münzel, T.; Feil, R.; Mülsch, A.; Lohmann, S.M.; Hofmann, F.; Walter, U. *Circulation* **2003**, 108, 2172-2183.
(8) Paolocci, N.; Katori, T.; Champion, H.C.; John, M.E.S.; Miranda, K.M.; Fukuto, J.M.; Wink, D.A.; Kass, D.A. *P. Natl. Acad. Sci. USA* **2003**, 100, 5537-5542.
(9) DeMaster, E.G.; Redfern, B.; Nagasawa, H.T. *Biochem. Pharmacol.* **1998**, 55, 2007-2015.
(10) A.J. Väänänen, P. Salmenperä, M. Hukkanen, P. Rauhala, E. Kankuri. *Free Radic. Bio. Med.* **2006**, 41, 120-131.
(11) Wink, D.A.; Miranda, K.M.; Katori, T.; Mancardi, D.; Thomas, D.D.; Ridnour, L.; Espey, M.G.; Feelisch, M.; Colton, C.A.; Fukuto, J.M.; Pagliaro, P.; Kass, D.A.; Paolocci, N. *Am. J. Phys. Heart C* **2003**, 285, 2264-2276.
(12) Fukuto, J.M.; Bartberger, M.D.; Dutton, A.S.; Paolocci, N.; Wink, D.A.; Houk, K. *Chem. Res. Toxicol.* **2005**, 18, 790-801.
(13) Espey, M.G.; Miranda, K.M.; Thomas, D.D.; Wink, D.A. *Free Radic. Bio. Med.* **2002**, 33, 827-834.
(14) Irvine, J.C.; Favaloro, J.L.; Kemp-Harper, B.K.; *Hypertension* **2003**, 41, 1301-1307.
(15) Zhang, M.; Han, H.-H.; Zhang, S.; Wang, C.; Lu, Y.; Zhu,W. *J. Mater.Chem. B.* **2017**, DOI: 10.1039/C7TB02323E.
(16) Wang, S.; Li, C.; Li, J.; Chen, B.; Guo, Y. *Acta Chim Sinica* **2017**, 75, 383-390.
(17) Cheng, D.; Pan, Y.; Wang, L.; Zeng, Z.; Yuan, L.; Zhang, X.; Chang, Y.-T. *J. Am. Chem. Soc.* **2016**, 139, 285-292.
(18) Wang, Y.-R.; Feng, L.; Xu, L.; Hou, J.; Jin, Q.; Zhou, N.; Lin, Y.; Cui, J.-N.; Ge, G.-B. *Sens. Actuators B* **2017**, 245, 923-931.
(19) Li, H.; Fan, J.; Peng, X. *Prog. Chem*. **2017**, 29, 17-35.
(20) Xu, Z.; Leng, S.; Qiao, Q.; Miao, L.; Deng, W.; Cui, J. *Chem. Commun.* **2017**, 53, 6448-6451.
(21) Wang, K.; Leng,T.; Liu, Y.; Wang, C.; Shi, P.; Shen, Y.; Zhu, W.-H. *Sens. Actuators B* **2017**, 248, 338-345.
(22) Zhang, W.; Liu, T.; Huo, F.; Ning, P.; Meng, X.; Yin, C. *Anal. Chem.* **2017**, 89, 8079-8083.
(23) Li, H.; Yao, Q.; Fan, J.; Hu, C.; Xu, F.; Du, J.; Wang, J.; Peng, X. *Ind. Eng. Chem. Res.* **2016**, 55, 1477-1483.
(24) Martí, M.A.; Bari, S.E.; Estrin, D.A.; Doctorovich, F. *J. Am. Chem. Soc.* **2005**, 127, 4680-4684.
(25) Cline, M.R.; Tu, C.; Silverman, D.N.; Toscano, J.P. *Free Radical Bio. Med.* **2011**, 50, 1274-1279.
(26) Samuni, U.; Samuni, Y.; Goldstein, S. *J. Am. Chem. Soc.* **2010**, 132, 8428-8432.
(27) Reisz, J.A.; Zink, C.N.; King, S.B. *J. Am. Chem. Soc.* **2011**, 133, 11675-11685.
(28) Suárez, S.N.A.; Bikiel, D.E.; Wetzler, D.E.; Martí, M.A.; Doctorovich, F. *Anal. Chem.* **2013**, 85, 10262-10269.
(29) Huo, Y.; Miao, J.; Han, L.; Li, Y.; Li, Z.; Shi, Y.; Guo, W. *Chem. Sci.* **2017**, 8, 6857-6864.
(30) Peng, J.; Samanta, A.; Zeng, X.; Han, S.; Wang, L.; Su, D.; Loong, D.T.B.; Kang, N.-Y.; Park, S.-J.; All, A.H.; Jiang, W.; Yuan, L.; Liu, X.; Chang, Y.-T. *Angew. Chem. Int. Edit*. **2017**, 56, 4165-4169.
(31) Li, D.; Xu, Y.; Zhou, N.; Liu, J.; Wang, R.; Cheng, T.; Tang, Y.; Zhu, W.; Xu, Y.; Qian, X. *Dyes Pigments*, **2017**, 136, 627-632.
(32) Chen, X.; Lim, C.S.; Lee, D.; Lee, S.; Park, S.J.; Kim, H.M.; Yoon, J. *Biosens. Bioelectron.* **2017**, 91, 770-779.
(33) Kim, E.-J.; Kumar, R.; Sharma, A.; Yoon, B.; Kim, H.M.; Lee, H.; Hong, K.S.; Kim, J.S. *Biomaterials* **2017**, 122, 83-90.
(34) Lv, J.; Wang, F.; Wei, T.; Chen, X. *Ind. Eng. Chem. Res.* **2017**, 56, 3757-3764.
(35) Li, H.; Yao, Q.; Fan, J.; Jiang, N.; Wang, J.; Xia, J.; Peng, X. *Chem. Commun.* **2015**, 51, 16225-16228.
(36) Tian, J.; Yan, Q.; Zhu, Y.; Zhang, J.; Li, J.; Shi, B.; Xu, G.; Fan, C.; Zhao, C. *Chinese J. Chem.* **2017**, DOI: 10.1002/cjoc.201700248.
(37) Li, H.; Yao, Q.; Fan, J.; Du, J.; Wang, J.; Peng, X. *Biosens. Bioelectron.* **2017**, 94, 536-543.
(38) Li, H.; Yao, Q.; Fan, J.; Du, J.; Wang, J.; Peng, X. D*yes Pigments*, **2016**, 133, 79-85.
(39) Rosenthal, J.; Lippard, S.J.; *J. Am. Chem. Soc.* **2010**, 132, 5536-5537.
(40) Rivera-Fuentes, P.; Lippard, S.J. *Acc. Chem. Res.* **2015**, 48, 2927-2934.
(41) Michael, M.A.; Pizzella, G.; Yang, L.; Shi, Y.; Evangelou, T.; Burke, D.T.; Zhang, Y. *J. Phys. Chem. Lett.* **2014**, 5, 1022-1026.
(42) Kim, S.; Minier, M.A.; Loas, A.; Becker, S.; Wang, F.; Lippard, S.J. *J. Am. Chem. Soc.* **2016**, 138, 1804-1807.
(43) Zhang, H.; Liu, R.; Tan, Y.; Xie, W.H.; Lei, H.; Cheung, H.-Y.; Su, H. *ACS Appl. Mater. Interfaces* **2015**, 7, 5438-5443.
(44) Sunwoo, K.; Bobba, K.N.; Lim, J.-Y.; Park, T.; Podder, A.; Heo, J.S.; Lee, S.G.; Bhuniya, S.; Kim, J.S. *Chem. Commun.* **2017**, 53, 1723-1726.
(45) Dong, B.; Song, X.; Kong, X.; Wang, C.; Zhang, N.; Lin, W. *J. Mater. Chem. B* **2017**, 5, 5218-5224.
(46) Gong, X.; Yang, X.-F.; Zhong, Y.; Chen, Y.; Li, Z. *Dyes Pigments*, **2016**, 131, 24-32.
(47) Zhu, X.; Xiong, M.; Liu, H.-W.; Mao, G.-J.; Zhou, L.; Zhang, J.; Hu, X.; Zhang, X.-B.; Tang, W. *Chem. Commun.* **2016**, 52, 733-736.

(48) Liu, C.; Cao, Z.; Wang, Z.; Jia, P.; Liu, J.; Wang, Z.; Han, B.; Huang, X.; Li, X.; Zhu, B.; Zhang, X. *Sens. Actuators B* **2015**, 220, 727-733.
(49) Jing, X.; Yu, F.; Chen, L. *Chem. Commun.* **2014**, 50, 14253-14256.
(50) Ren, M.; Deng, B.; Zhou, K.; Wang, J.-Y.; Kong, X.; Lin, W. *J. Mater. Chem. B.* **2017**, 5, 1954-1961.
(51) Liu, C,; Wang, Y.; Tang, C.; Liu, F.; Ma, Z.; Zhao, Q.; Wang, Z.; Zhu, B.; Zhang, X. *J. Mater. Chem. B.* **2017**, 5, 3557-3564.
(52) Wrobel, A.T.; Johnstone, T.C.; Liang, A.D.; Lippard, S.J. *J. Am. Chem. Soc.* **2014**, 136, 4697-4705.
(53) Mao, G.-J.; Zhang, X.-B.; Shi, X.-L.; Liu, H.-W.; Wu, Y.-X.; Zhou, L.-Y.; Tang, W.; Yu, R.-Q. *Chem. Commun*. **2014**, 50, 5790-5792.
(54) Liu, P.; Jing, X.; Yu, F.; Lv, C.; Chen, L. *Analyst* **2015**, 140, 4576-4583.
(55) Zeng, L.; Chen, S.; Xia, T.; Hu, W.; Li, C.; Liu, Z. *Anal. Chem.* **2015**, 87, 3004-3010.
(56) Zhang, J.; Liu, H.-W.; Hu, X.-X.; Li, J.; Liang, L.-H.; Zhang, X.-B.; Tang, W. *Anal. Chem.* **2015**, 87, 11832-11839.
(57) C.H. Heo, A.R. Sarkar, S.H. Baik, T.S. Jung, J.J. Kim, H. Kang, I. Mook-Jung, H. M. Kim. *Chem. Sci.* **2016**, 7, 4600-4606.
(58) Dong, X.; Heo, C.H.; Chen, S.; Kim, H.M.; Liu, Z. *Anal. Chem.* **2013**, 86, 308-311.
(59) Mao, Z.; Hu, L.; Dong, X.; Zhong, C.; Liu, B.-F.; Liu, Z. *Anal. Chem.* **2014**, 86, 6548-6554.
(60) Hu, W.; Zeng, L.; Wang, Y.; Liu, Z.; Ye, X.; Li, C. *Analyst* **2016**, 141, 5450-5455.
(61) Suarez, S.A.; Neuman, N.I.; Muñoz, M.; Álvarez, L.a.; Bikiel, D.E.; Brondino, C.D.; Ivana, I.B.; Miljkovic, J.L.; Filipovic, M.R.; Martí, M.A.; Doctorovich, F. *J. Am. Chem. Soc*. **2015**, 137, 4720-4727.

For TOC Only